

Microwave Synthesis of Water-Dispersed CdTe/CdS/ZnS Core-Shell-Shell Quantum Dots with Excellent Photostability and Biocompatibility**

By Yao He, Hao-Ting Lu, Li-Man Sai, Yuan-Yuan Su, Mei Hu, Chun-Hai Fan, Wei Huang,* and Lian-Hui Wang*

In the past decades, colloidal luminescent semiconductor nanocrystals, often referred to as quantum dots (QDs), attracted much attention due to their unique advantages over traditional fluorescent dyes, such as size-tunable emission, broad photoexcitation combined with narrow photoemission, strong fluorescence, and high resistance to photobleaching.^[1] It is well-known that high quality, water-dispersed QDs, i.e., QDs with a high photoluminescent quantum yield (PLQY), narrow full-width at half maximum (fwhm), excellent photostability, and favorable biocompatibility, are promising for many biological applications.^[2] Different kind of highly luminescent QDs can be prepared via organometallic routes, e.g., CdSe, CdSe/ZnS core-shell (CS), and CdSe/CdS/ZnS core-shell-shell (CSS) QDs with high PLQY (40–80%) which were successfully prepared in an organic phase.^[3] However, complicated manipulations are required to disperse these QDs in water, e.g., wrapping an amphiphilic polymer around the QDs or substituting the hydrophilic molecules for surface-binding TOPO molecules.^[4] Moreover, the PLQY often decreases when QDs are transferred to water because the polarity of the water is so strong that it breaks various equilibriums related to the QDs.^[5] Nevertheless, water-dispersed QDs can be directly synthesized via an aqueous method, which is simpler, cheaper, and less toxic, but generally poor-quality QDs (PLQY lower than 30%) are obtained via this method.^[6] From 2003 onwards, several effective strategies were deployed to directly prepare QDs in the aqueous phase.^[7] For example, highly luminescent CdTe and CdTe/CdS CS QDs were recently successfully

synthesized via microwave irradiation by our group.^[8] However, an inherent cytotoxicity is observed when Cd²⁺ ions are desorbed from the QDs, particularly under UV irradiation.^[9] To the best of our knowledge, no thiol-stabilized QDs have been reported to date, which were directly prepared in the aqueous phase and possess both excellent photostability and favorable biocompatibility. As a consequence, further bioapplications were held back even though these QDs have the advantage of being non-blinking over those prepared via organic routes.^[10]

In this communication, we present the first example of water-dispersed CdTe/CdS/ZnS CSS QDs which are synthesized in the aqueous phase assisted by microwave irradiation (Fig. 1a). As-prepared CSS QDs do not only possess a high PLQY (40–80%) but also exhibit excellent photostability (17-fold more stable than bare CdTe QDs) and favorable biocompatibility (non-cytotoxic to K562 cells at 3 μM and up to 48 h incubation). If the ZnS shell was grown directly on to the surface of CdTe QDs, serious strain would be generated between CdTe and ZnS due to their large lattice mismatch (16.4%), which leads to low PLQYs and broad size distributions, as shown in Figure 1b.^[3a,3b] On the basis of this analysis, a CdS shell, whose band gap energy and lattice constant is between those of CdTe and ZnS, was introduced as a buffer layer between the CdTe core and the ZnS shell in this work. This double shell structure allows a stepwise change of lattice spacing from the emitting CdTe core to the protecting ZnS shell, which reduces the strain within the QD.^[3b] Moreover, charge carriers are effectively confined within the core region and separated from the surface due to the adequate offset of band gap energies ($\sim 2\text{ eV}$) between core and double-shell region. This reduces non-radiative surface defects and improved the PLQY.^[3b,11] Considering that highly luminescent CdTe/CdS CS QDs have successfully been prepared in an aqueous phase despite their relatively large lattice mismatch (10.0%),^[8b] the ZnS shell is expected to exhibit well-defined epitaxial growth on the surface of the CdS shell due to the smaller lattice mismatch (6.4%).

Figure 1c displays the representative UV-vis absorption and photoluminescence (PL) spectra of CdTe core QDs, CdTe/CdS CS QDs, and corresponding CdTe/CdS/ZnS CSS QDs synthesized by microwave irradiation. In both spectra, a red-shift is observed for CSS QDs compared to core QDs and CS QDs, which is an indication for the formation of the intended CdTe/

[*] Prof. L.-H. Wang, Dr. Y. He, H.-T. Lu, L.-M. Sai, M. Hu
Laboratory of Advanced Materials, Fudan University
Shanghai, 200433 (PR China)
E-mail: wlhui@fudan.edu.cn

Prof. W. Huang
Institute of Advanced Materials, Nanjing University of Posts and
Telecommunication
Nanjing, 210003 (PR China)
E-mail: wei-huang@njupt.edu.cn

Dr. Y.-Y. Su, Prof. C.-H. Fan
Chinese Academy of Sciences, Shanghai Institute of Applied Physics
Shanghai, 201800 (PR China)

[**] This work was financially supported by the National Natural Science Foundation of China under Grants 30425020, 90406021, and 60537030, as well as the Shanghai Commission of Education under Grant 2004SG06, and the Shanghai Leading Academic Discipline Project, Project No. B113.

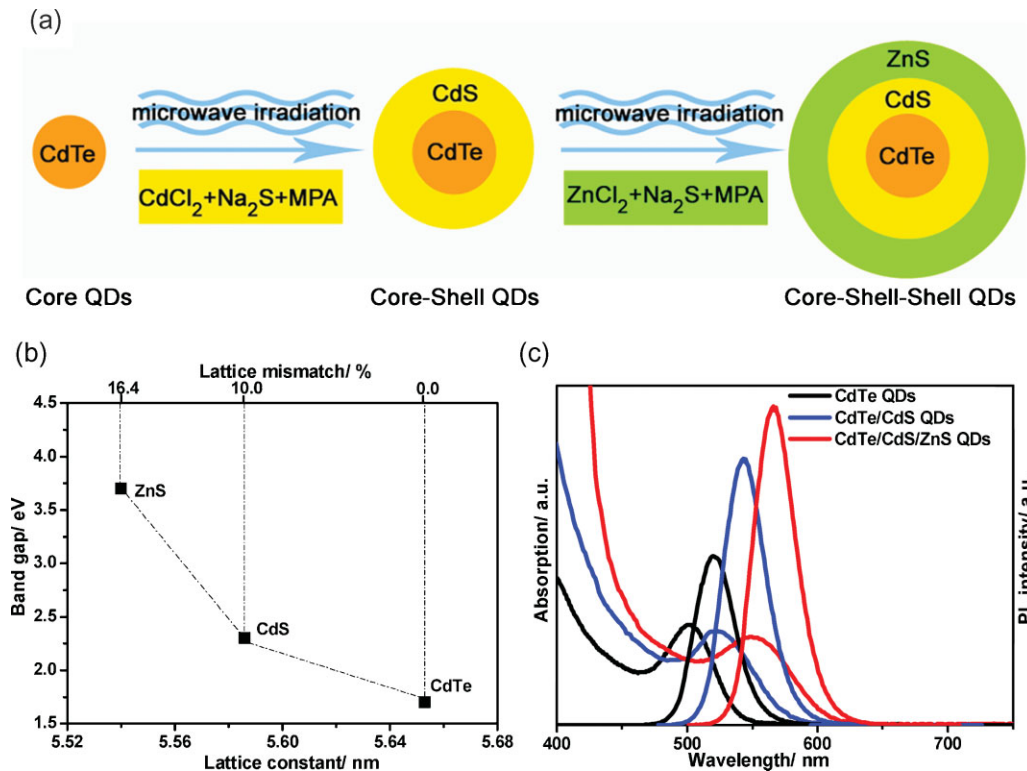


Figure 1. a) Schematic illustration of microwave (MW)-assisted synthesis of water-dispersed CdTe/CdS/ZnS core-shell-shell (CSS) quantum dots (QDs). b) Interrelationship between band gap energy, lattice constant, and lattice mismatch of bulk CdTe, CdS, and ZnS. Herein, lattice mismatch refers to the mismatch compared to CdTe. c) Representative absorption and photoluminescence (PL) spectra of CdTe core QDs (photoluminescence quantum yield (PLQY) ~30%), CdTe/CdS core-shell QDs (PLQY ~65%), and corresponding CdTe/CdS/ZnS core-shell-shell QDs (PLQY ~80%) prepared at 100 °C and 1 min MW irradiation, 100 °C/5 min, and 60 °C/5 min, respectively.

CdS/ZnS CSS structure rather than a Cd_xZn_{1-x}Te_yS_{1-y} alloy. The formation of alloyed QDs would lead to a blue shift in both UV-vis absorption and PL spectrum because of the larger band-gap energy of alloyed QDs.^[8b,13] It is worth mentioning, that the temperature is of utmost importance during the formation of the ZnS shell on the CdTe/CdS QDs. As reported previously, excessive temperatures cause broad size distributions, large amount of surface defects, and are adverse to the spectral properties of QDs.^[8] Consequently, the relatively low temperatures used in the current research (60–70 °C) were favorable for the good epitaxial growth of a ZnS shell with a high degree of crystallinity. Additionally, the PL intensity of as-prepared QDs was superior to that of corresponding CdTe/CdS QDs, since the ZnS shell effectively reduced the number of defects on the surface of the QDs.^[3c] As a result, highly luminescent (PLQY 40–80%) CdTe/CdS/ZnS CSS QDs in a range of sizes (λ_{max} = 530–615 nm) were prepared using microwave irradiation (Fig. 2).

Figure 3 shows transmission electron microscopy (TEM) and high-resolution TEM (HRTEM) images of the as-prepared CdTe core (PLQY ~40%), CdTe/CdS CS (PLQY ~65%), and CdTe/CdS/ZnS CSS QDs (PLQY ~80%) whereby the observed increment in size results from the growth of the first (CdS) and the second (ZnS) shell. Furthermore, HRTEM images of the core, CS, and CSS QDs show obvious lattice

planes that extend across the entire particle with no evidence of an interface between the core and shells, which is consistent with a coherent epitaxial growth mechanism and demonstrates that the shell growth does not disturb the crystalline form of the core.^[3,8b] In comparison to that of CdTe QDs (2.6 nm), the size of CS or CSS QDs increased to 3.7 or 4.5 nm, respectively, which indicates an optimal thickness of 1.1 or 0.8 nm for the CdS or ZnS shell, respectively.

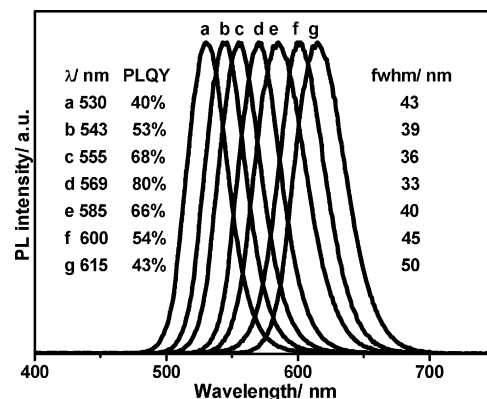


Figure 2. PL spectra of synthesized CdTe/CdS/ZnS core-shell-shell QDs with a series of maximum emission wavelengths. Related PLQY and full width at half maximum (fwhm) values are presented.

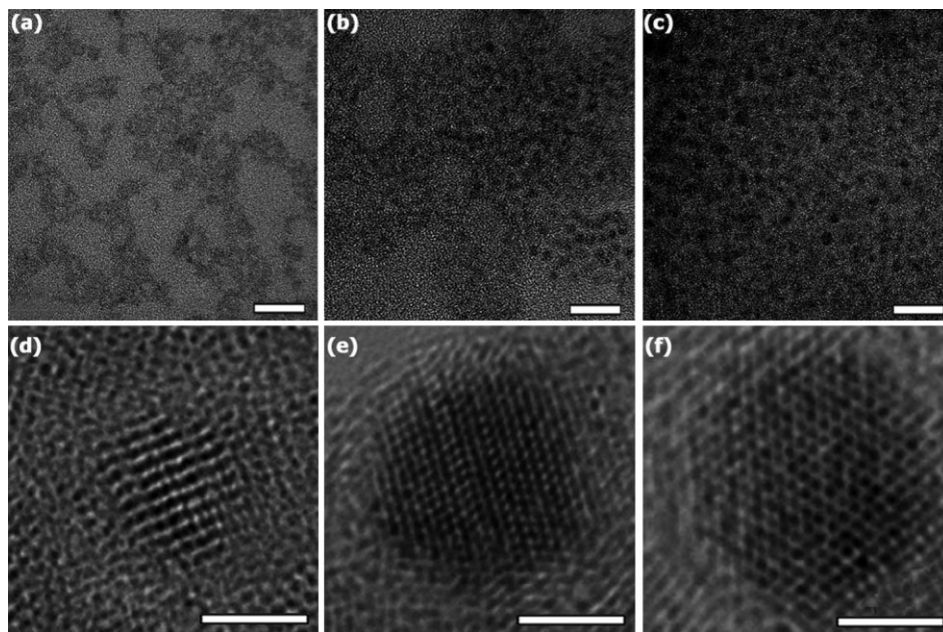


Figure 3. Transmission electron microscopy (TEM, top) and high-resolution (HR) TEM (bottom) images of a), d) CdTe core QDs; b), e) CdTe/CdS core-shell QDs; and c), f) CdTe/CdS/ZnS core-shell-shell QDs synthesized using microwave irradiation. Scale bars are 20 nm (a–c) and 2 nm (d–f), respectively.

Powder X-ray diffraction (XRD) and X-ray photoelectron spectroscopy (XPS) analysis results for CdTe core, CdTe/CdS CS, and CdTe/CdS/ZnS CSS QDs solid samples that were precipitated from the aqueous solution with an excess of 2-isopropanol are shown in Figure 4. Figure 4a shows that the diffraction of bare CdTe QDs is quite close to that of bulk cubic CdTe. In contrast, the diffraction patterns of CS and CSS QDs shift to higher angles, accompanied by the emergence of CdS and ZnS phases due to the growth of the CdS and ZnS shells,

while the pattern of peak widths and shapes is nearly unchanged, which further demonstrates the formation of CS and CSS structures rather than an alloyed structure. A homogeneous alloy would show a significant narrowing of XRD peak widths upon increasing particle size.^[3] The distribution of bond lengths resulting from intrinsic stains is a possible explanation for why the XRD peak widths and shapes of the CS and CSS QDs are approximate with those of the core QDs.^[8b,14]

The XPS results further confirm the proposed CS and CSS structures. As shown in Figure 4b, the coordination of Cd-S in CdTe/CdS QDs is different to that of Cd-SR (i.e., thiols) in CdTe QDs. As a result, the binding energy assigned to S2p3 shifts from 162 eV in CdTe/CdS QDs to 164 eV in CdTe QDs, which verifies the proposed core-shell structure and is consistent with previous reports.^[8b,15] The emergence of new Zn3p3, Zn Auger, and Zn2p peaks in the CdTe/CdS/ZnS QDs XPS spectrum, which are attributed to Zn from the ZnS, further validates the proposed core-shell-shell structure in which ZnS acts as the second shell encapsulating the CdTe core QDs. The relative concentration of Te, Cd, S, and Zn in the CdTe/CdS/ZnS QDs is 7.6%, 25.7%, 43.2%, and 23.5%, respectively, which was calculated by dividing the area of each XPS peak by its respective sensitivity factor.^[3a]

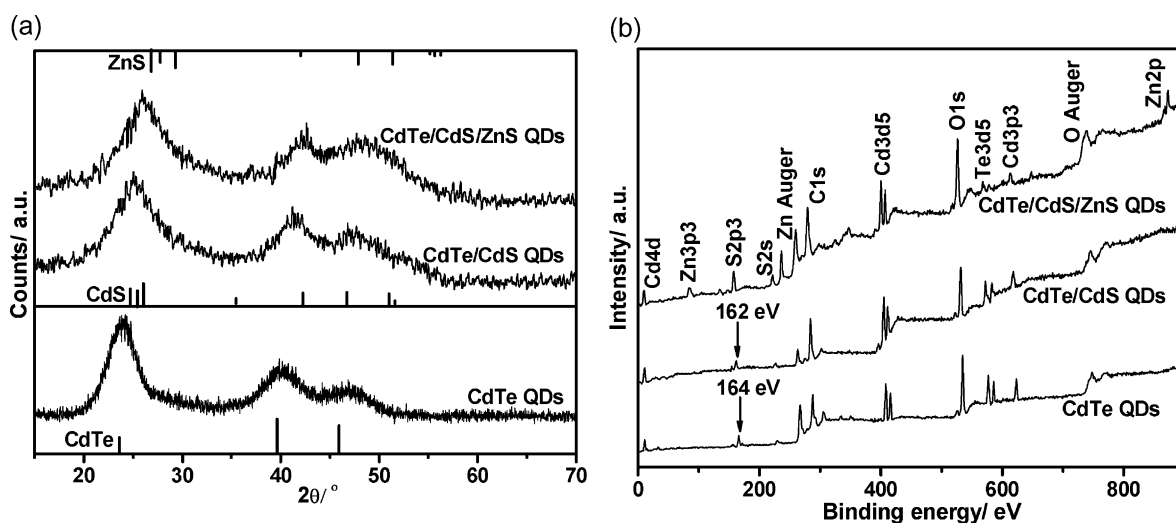


Figure 4. a) Powder X-ray diffraction (XRD) patterns of CdTe core QDs, CdTe/CdS core-shell QDs, and corresponding CdTe/CdS/ZnS core-shell-shell QDs. Standard diffraction lines of cubic CdTe, cubic CdS, and cubic ZnS are shown for comparison. b) X-ray photoelectron spectra (XPS) of the same materials.

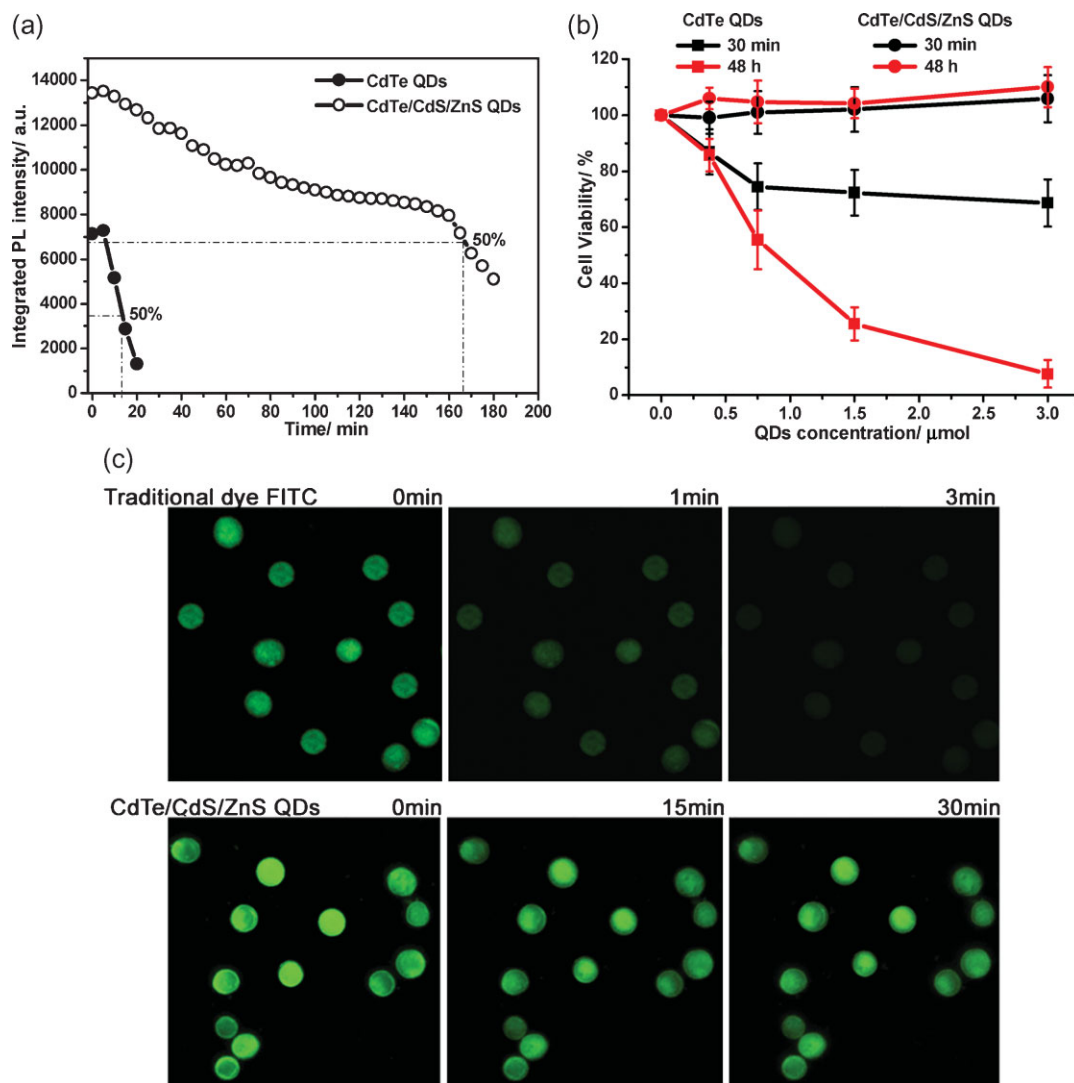


Figure 5. a) Evolution of the integrated PL intensity of oxygen-saturated solutions of CdTe and the CdTe/CdS/ZnS QDs under irradiation (Xenon lamp, 365 nm, 450 W). b) Cytotoxicity of different concentrations of CdTe and CdTe/CdS/ZnS QDs in K562 cells. c) Comparison of the photostability of fluorescein isothiocyanate (FITC) and CdTe/CdS/ZnS QDs upon staining of ethanol-fixed K562 cells.

Bare CdTe QDs easily aggregate under UV irradiation.^[6] As shown in Figure 5a, their integrated PL intensity rapidly decreases in only 5 min, after which they are completely aggregated and precipitate out of solution within ~20 min. Comparatively, the photostability of as-prepared CSS QDs was significantly improved. Although a slight decline of PL intensity was observed upon UV irradiation, it still remained at 50% of the initial value after up to 170 min irradiation under the same conditions. The reason is that the double shell effectively protects the core QDs from the UV irradiation and as a consequence unsaturated Te atoms on the surface of the core are not oxidized by the UV irradiation.^[3b,12] In addition, these CSS QDs are extremely stable and do not change their optical properties for months when stored at ambient conditions without N₂-protection. Moreover, as-prepared QDs were used

to stain ethanol-fixed human K562 cells. Irradiated by UV light the QDs within the cells produced a bright olivine color, which retained the same PL intensity even after 30 min irradiation (Fig. 5c). In comparison, fluorescent signals of cells stained with FITC, a dye traditionally used as bio-fluorescent agent, were nearly invisible after merely 3 min irradiation due to severe photobleaching, which is characteristic for FITC. In addition, the fluorescent intensity of FITC was weaker even at a concentration 30 times higher than that of as-prepared CSS QDs.

Another critical characteristic for future biological applications is the biocompatibility of QDs, especially for clinical applications. Thorough research revealed that the liberation of toxic Cd²⁺ ions from QDs and the tendency of QDs to aggregate in living cells are two significant factors that lead to their

cytotoxicity.^[9,12] Therefore, polymer coats or epitaxially grown ZnS shells on the surface of QDs are feasible strategies to improve the biocompatibility of QDs.^[9a,12] For that reason, we deduced that the double-shell structure QDs were much more biocompatible than the bare CdTe QDs. With an aim to validate this hypothesis, the cytotoxicity of CdTe QDs and CSS QDs was elaborately studied at various concentrations. As shown in Figure 5b, CSS QDs were non-cytotoxic to leukaemia K562 cells in concentrations of up to 3 μM after 48 h incubation, whereas the cell viability drastically decreased when the cells were incubated with bare CdTe QDs instead, even at a concentration as low as 0.375 μM . The reason being that Cd^{2+} ions released from the relatively unstable CdTe QDs are incredibly cytotoxic.^[9,12]

In conclusion, we demonstrated for the first time the synthesis of CdTe/CdS/ZnS CSS QDs in aqueous phase assisted by microwave irradiation. These QDs do not only possess a high PLOY but also excellent photostability and favorable biocompatibility, which is vital for many biological applications. Therefore, this class of water-dispersed CSS QDs is a promising candidate for fluorescent probes in biological and medical fields, some of which are currently under investigation and results thereof will be reported in the near future.

Experimental

Synthesis of CdTe core QDs, CdTe/CdS CS QDs, and CdTe/CdS/ZnS CSS QDs: Tellurium powder (99.9%), CdCl_2 (99.9%), and FTIC ($1 \text{ mg} \cdot \text{mL}^{-1}$) were purchased from Aldrich. 3-Mercaptopropionic acid (MPA, 98%), Rhodamine 590, Rhodamine B, and Rhodamine 640 were purchased from Fluka. NaBH_4 (99%), Na_2S (99%), ZnCl_2 (99%), and ethanol (99%) were obtained from Shanghai Chemical Reagents Company. All chemicals were used without further purification. Solutions were prepared using Milli-Q water (Millipore) as the solvent. K562 cells were cultured in Dulbecco's modified Eagle's Medium (DMEM), supplemented with 10% heat-inactivated fetal bovine serum (FBS) and antibiotics ($100 \mu\text{g} \cdot \text{mL}^{-1}$ streptomycin, $100 \mu\text{g} \cdot \text{mL}^{-1}$ penicillin), at 37 °C in a humidified atmosphere with 5% CO_2 . The microwave system (Version 3.5.7) used for the synthesis of CdTe QDs, CdTe/CdS CS QDs, and CdTe/CdS/ZnS CSS QDs was manufactured by CEM, USA. Vitreous vessels with a volume of 10 or 100 mL were used as reaction vessels during reactions demanding high temperature and pressure. UV-vis absorption spectra were obtained using a Shimadzu UV-3150 UV-vis-near-infrared spectrophotometer. Fluorescence spectra were collected on a Shimadzu RF-6301PC spectrofluorometer. All optical measurements were performed at room temperature under ambient conditions. X-ray diffraction (XRD) patterns were obtained using a Rigaku D/max- γ B diffractometer. X-ray photoelectron spectroscopy (XPS) was carried out using a PHI 5000C ESCA System (RBD, USA); corresponding data was analyzed through a AugerScan3.21 software. Transmission electron microscopy (TEM) and high-resolution (HR) TEM images were recorded on a JEOL JEM 2011 electron microscope and a Philips CM 200 electron microscope operated at 200 kV, respectively. The MTT assay for cell viability measurements was read on an ELISA reader (Model-680, BIO-RAD, USA). Fluorescence images of cells stained with QDs or FITC were taken on an Axioskop2 fluorescence microscope (ZEISS, Germany). Highly luminescent CdTe and CdTe/CdS CS QDs were prepared according to our previously published reports^[8b]. Briefly, a CdTe precursor solution was prepared by adding freshly prepared NaHTe solution to a N_2 -saturated CdCl_2 solution (pH 8.4) in the

presence of the stabilizer 3-mercaptopropionic acid (MPA). Cd, MPA, and Te precursor concentrations were 1.25 mM, 3.0 mM, and 0.625 mM, respectively. The CdTe precursor solution (50 mL) was injected into a vitreous vessel. CdTe QDs (photoluminescence quantum yield (PLOY) $\sim 30\%$) with a maximum emission wavelength of $\sim 520 \text{ nm}$ were obtained after 1 min microwave irradiation of the precursor solution at 100 °C. A CdTe QDs sample was taken when the temperature cooled down to $<50 \text{ }^\circ\text{C}$. The as-prepared CdTe solution was concentrated to $\frac{1}{4}$ of the original volume and CdTe QDs were precipitated with 2-propanol and collected via centrifugation. The colloidal precipitate was re-dissolved in ultrapure water (3 mL) and used as CdTe core QDs in subsequent steps. The CdTe/CdS precursor solution was prepared by adding the as-prepared CdTe core QDs to a N_2 -saturated solution containing 1.25 mM CdCl_2 , 1.0 mM Na_2S , and 6.0 mM MPA (pH 8.4). The CdTe/CdS precursor solution (50 mL) was injected into a vitreous vessel. CdTe/CdS core-shell QDs (PLOY $\sim 65\%$) with a maximum emission wavelength of $\sim 545 \text{ nm}$ were obtained after 5 min microwave irradiation of the precursor solution at 100 °C. A CdTe/CdS sample was taken when the temperature cooled down to $<50 \text{ }^\circ\text{C}$. The as-prepared CdTe/CdS solution was concentrated to $\frac{1}{4}$ of the original volume and CdTe/CdS QDs were precipitated with 2-propanol and collected via centrifugation. The colloidal precipitate was re-dissolved in 3 mL ultrapure water and used as CdTe/CdS core-shell (CS) QDs in subsequent steps.

The CdTe/CdS/ZnS precursor solution was prepared by adding the as-prepared CdTe/CdS CS QDs to a N_2 -saturated solution containing 1.25 mM ZnCl_2 , 1.0 mM Na_2S , and 6.0 mM MPA (pH 8.4). The CdTe/CdS/ZnS precursor solution (4 mL) was injected into a vitreous vessel and irradiated with MW for 5 min at 60 °C. CdTe/CdS/ZnS core-shell-shell QDs (PLOY $\sim 80\%$) with a maximum emission wavelength of $\sim 565 \text{ nm}$ were obtained. A CdTe/CdS/ZnS sample was taken when the temperature cooled down to $<50 \text{ }^\circ\text{C}$. Various sizes of highly luminescent CdTe/CdS/ZnS QD ($\lambda_{\text{max}} = \sim 530\text{--}610 \text{ nm}$, PLOY $\sim 40\text{--}80\%$) can be realized upon manipulation of the size of the CdTe core or CdTe/CdS core-shell QDs, and duration of microwave irradiation. No post-synthesis treatment was performed on any of the samples used for optical characterizations. Samples were precipitated using 2-propanol and dried in a vacuum oven prior to XRD and XPS characterization. TEM and HRTEM samples were prepared by dropping the aqueous QD solutions onto carbon-coated copper grids and evaporating any excessive solvent. The PLOY was estimated at room temperature using Rhodamine 590, Rhodamine B, and Rhodamine 640 in ethanol according to the different maximum emission wavelengths of the QDs [16].

Comparison of the photostability of CdTe core QDs and CdTe/CdS/ZnS CSS QDs: With the aim to exclude the influence of residual reagents, e.g., MPA, Cd^{2+} , Te^{2-} , and Zn^{2+} , the comparison was carried out after strictly post-treatment. In detail, 2-propanol was added dropwise to the QD solutions under stirring until the sample solutions became slightly turbid. The turbid dispersions were then stirred for further 15 min. A first sample fraction was collected by centrifugation. Another portion of 2-propanol was added dropwise to the supernatant to obtain the second fraction of sample and so on. This procedure was repeated three times before one fraction of the CdTe core QDs and one of the corresponding CdTe/CdS/ZnS QDs were selected for comparison. Both fractions were washed with Milli-Q water three times to adequately remove any residual reagent from the samples and were diluted to give an absorption value of ~ 0.1 at the excitation wavelength of CdTe core and CdTe/CdS/ZnS Core-shell-shell QDs, respectively. Finally, the diluted samples were irradiated with a 350 W Xe lamp (365 nm) for different time intervals.

Staining of fixed K562 cells using CdTe/CdS/ZnS CSS QDs and imaging of the stained cells: Similar manipulations were described elsewhere [17]. Briefly, 5,000 K562 cells (2 mL culture medium) were fixed with ethanol (400 μL , 75%) and washed with PBS three times. Thereafter, cells were incubated in 1% BSA solution in PBS for 30 min at 25 °C and then in CdTe/CdS/ZnS CSS QDs solution (20 μL , 3 μL) for 15 min at 25 °C, before being washed with PBS three times to remove

any unbound QDs (QD concentration was calculated according to [12b]). Stained cells were imaged with a fluorescence microscope using UV excitation. In the case of FITC being used as stain, all manipulations were identical to those mentioned above. However the concentration of FITC was increased to 90 μM and the incubation prolonged to 45 min.

Comparison of the cytotoxicity of CdTe core QDs and CdTe/CdS/ZnS CSS QDs: K562 cells (in DMEM Medium) were dispensed in 96-well plates (90 μL per well containing 3×10^4 cells). Serial dilutions of CdTe QDs were prepared in Milli-Q water and added to each well (10 μL). Concentrations were calculated following a previously published method by Yu et al. [18]. Cells were incubated at 37 °C in a humidified atmosphere with 5% CO_2 for 2, 6, or 24 h after which the cytotoxicity of the CdTe QDs was evaluated using an MTT assay (3-(4,5-dimethylthiazol-2-yl)-2,5-diphenyltetrazolium bromide, Thiazolyl blue tetrazolium bromide, M5655, Sigma). The assay is based on the accumulation of dark blue formazan crystals inside living cells after their exposure to MTT. Addition of sodium dodecylsulfate (SDS) results in a disruption of the cell membrane and subsequent liberation and solubilisation of the crystals. The number of viable cells is thus directly proportional to the level of formazan product created. The formazan concentration is finally quantified using a spectrophotometer by measuring the absorbance at 570 nm (ELISA reader). A linear relationship between cell number and optical density is established, thus allowing an accurate quantification of changes in the rate of cell proliferation. Identical manipulations were used when CdTe/CdS/ZnS CSS QDs were substituted for CdTe QDs.

Received: May 14, 2007

Revised: January 3, 2008

Published online: August 5, 2008

- [1] a) M. P. Bruchez, M. Moronne, P. Gin, S. Weiss, A. P. Alivisatos, *Science* **1998**, *281*, 2013. b) W. C. W. Chan, S. M. Nie, *Science* **1998**, *281*, 2016. c) Q. J. Sun, Y. A. Wang, L. S. Li, D. Y. Wang, T. Zhu, J. Xu, C. H. Yang, Y. F. Li, *Nat. Photonics* **2007**, *1*, 717.
- [2] X. Michalet, F. F. Pinaud, L. A. Bentolila, J. M. Tsay, S. Doose, J. J. Li, G. Sundaresan, A. M. Wu, S. S. Gambhir, S. Weiss, *Science* **2005**, *307*, 538.
- [3] a) B. O. Dabbousi, J. Rodriguez-Viejo, F. V. Mikulec, J. R. Heine, J. R. Mattoussi, R. Ober, K. F. Jensen, M. G. Bawendi, *J. Phys. Chem. B* **1997**, *101*, 9463. b) D. V. Talapin, I. Mekis, S. Gotzinger, A. Kornowski, O. Benson, H. Weller, *J. Phys. Chem. B* **2004**, *108*, 18826. c) L. Qu, X. G. Peng, *J. Am. Chem. Soc.* **2002**, *124*, 2049.
- [4] a) D. Gerion, F. Pinaud, S. C. Williams, W. J. Parak, D. Zanchet, S. Weiss, A. P. Alivisatos, *J. Phys. Chem. B* **2001**, *105*, 8861. b) T. Pellegrino, L. Manna, S. Kudera, T. Liedl, D. Koktysh, A. L. Rogach, S. Keller, J. Radler, G. Natile, W. J. Parak, *Nano Lett.* **2004**, *4*, 703.
- [5] S. F. Wuister, I. Swart, F. V. Driel, S. G. Hickey, C. M. Donega, *Nano Lett.* **2003**, *3*, 503.
- [6] N. Gaponik, D. Talapin, A. L. Rogach, K. Hoppe, E. Shevchenko, A. Kornowski, A. Eychmuller, H. Weller, *J. Phys. Chem. B* **2002**, *106*, 7177.
- [7] a) H. Zhang, L. P. Wang, H. M. Xiong, L. H. Hu, B. Yang, W. Li, *Adv. Mater.* **2003**, *15*, 1712. b) L. Li, H. F. Qian, J. C. Ren, *Chem. Commun.* **2005**, 528.
- [8] a) Y. He, H. T. Lu, L. M. Sai, W. Y. Lai, Q. L. Fan, L. H. Wang, W. Huang, *J. Phys. Chem. B* **2006**, *110*, 13352. b) Y. He, H. T. Lu, L. M. Sai, W. Y. Lai, Q. L. Fan, L. H. Wang, W. Huang, *J. Phys. Chem. B* **2006**, *110*, 13370. c) Y. He, L. M. Sai, H. T. Lu, M. Hu, W. Y. Lai, Q. L. Fan, L. H. Wang, W. Huang, *Chem. Mater.* **2007**, *19*, 359.
- [9] a) V. A. Sianni, D. S. Koktysh, B. G. Yun, R. L. Matts, T. C. Pappas, M. Motamedi, S. N. Thomas, N. A. Kotov, *Nano Lett.* **2003**, *3*, 1177. b) A. M. Derfus, W. C. W. Chan, S. N. Bhatia, *Nano Lett.* **2004**, *4*, 11.
- [10] H. He, H. F. Qian, C. Q. Dong, K. L. Wang, J. C. Ren, *Angew. Chem. Int. Ed.* **2006**, *45*, 7588.
- [11] A. Aharoni, T. Mokari, I. Popov, U. Banin, *J. Am. Chem. Soc.* **2006**, *128*, 257.
- [12] a) A. Hoshini, K. Fujioka, T. Oku, M. Suga, Y. F. Sasaki, T. Ohta, M. Yasuhara, K. Suzuki, K. Yamamoto, *Nano Lett.* **2004**, *11*, 2163. b) C. Kirchner, T. Liedl, S. Kudera, T. Pellegrino, A. M. Javier, H. E. Gaub, S. Stolzle, N. Fertig, W. J. Parak, *Nano Lett.* **2005**, *5*, 331.
- [13] a) I. Mekis, D. V. Talapin, A. Kornowski, M. Haase, H. Weller, *J. Phys. Chem. B* **2003**, *107*, 7454. b) D. Pan, Q. Wang, S. Jiang, X. Ji, L. An, *Adv. Mater.* **2005**, *17*, 176.
- [14] X. G. Peng, M. C. Schlamp, A. V. Kadavanich, A. P. Alivisatos, *J. Am. Chem. Soc.* **1997**, *119*, 7019.
- [15] H. B. Bao, Y. J. Gong, Z. Li, M. Y. Gao, *Chem. Mater.* **2004**, *16*, 3853.
- [16] a) G. A. Grosby, J. N. J. Demas, *J. Phys. Chem.* **1971**, *75*, 991. b) L. Qu, X. G. Peng, *J. Am. Chem. Soc.* **2002**, *124*, 2049.
- [17] J. K. Jaiswal, E. R. Goldman, H. Mattoussi, S. M. Simon, *Nat. Methods* **2004**, *1*, 73.
- [18] W. W. Yu, L. Qu, W. Guo, X. G. Peng, *Chem. Mater.* **2003**, *15*, 2854.